Performance Investigation of GaSb/Si Heterojunction based Gate Underlap and Overlap Vertical TFET Biosensor

A.Theja and Meena Panchore*, *Member, IEEE*

***Abstract*—The present paper estimates the performance of vertically developed double gate GaSb/Si tunnel field-effect transistor (V-DGTFET) biosensor with source pocket. A commercially accessible tool, Silvaco-TCAD, is exploited for carrying simulations of V-DGTFET. The device's novelty is deploying a material with a small bandgap, namely GaSb, in the source region to improve the carrier tunneling in source-channel (GaSb-Si) heterojunction. Further, the present work has analysed the performance on half gate underlap and half gate overlap V-DGTFET based label-free biosensor. The performance of V-DGTFET biosensor corresponding to various biomolecules such as APTES with κ=3.57, bacteriophage-T7 with κ=6.4, apomyoglobin with κ =8.1 and gelatin with κ=12 is investigated with reference to energy band diagram, potential profile, electric field and drain characteristics. Furthermore, by considering the different values of dielectric constants from 1 to 12, the present paper computed the figure of merits (FOMs) essentially linearity and sensitivity. The results demonstrated that neutral biomolecules with higher dielectric constant values showed higher sensitivity compared with other biomolecules. Moreover, it is estimated that gelatin has to drain current sensitivity of 5.6×10^5, which is 13%, 20%, and 41% more in comparison to apomyoglobin (κ =8.1), bacteriophage-T7 (κ=6.4), and APTES (κ =3.57) sensitivity at 15 nm cavity length.**

***Index Terms*- Vertical double gate tfet(V-DGTFET), heterojunctions, poisson's equation, parabolic approximation, subthreshold swing (SS), gate underlap, gate overlap.**

I. Introduction

Recently, the research community has given considerable attention to biosensors for label-free identification of biological particles such as proteins, glucose, and antibodies [1]. Biosensors have been used in medical diagnosis, monitoring environmental conditions, the agriculture domain, and criminal identification [2]. Considering different potential devices available for bio-sensing functions, the field-effect transistor shows classic performance as a label-free biosensor. Since FETs are more compatible with MOS devices, they have higher scalability, are cost-effective, and have ultra-sensitivity [3]–[5]. However, FET-based biosensors have many advantages, but they also have substantial drawbacks. For example, scaling challenges and short channel effects (SECs) are experienced by the FET during the downsizing process. Also, there is a theoretical limitation on the minimal subthreshold swing (SS >60 mV/dec) [6]–[9], which leads to slower response time in the detection of biomolecules. These difficulties degrade the efficiency and sensitivity of the device, and thermionic electron emission in FETs leads to excessive power dissipation. To overcome these issues, researchers are turning their attention to TFET-based biosensors. Because of carrier band to band tunnelling (BTBT) they exhibit low power consumption and excellent electrical characteristics. Further, in TFETs, there is an effective coupling at the tunnel junction in the presence of biomolecules inside the cavity, which results in high sensitivity. Also, TFETs are more scalable and resistant to sensitivity degradation at lower dimensions, unlike FETs. Furthermore, the smaller size, lower cost, and mass production capacity are the most significant characteristics of TFET based biosensors [10]. Therefore, the TFET based biosensors are preferred over others.

In compared to conventional MOSFETs, the TFETs exhibit much lower OFF current (I_{OFF}), decreased sub-threshold swing (SS<60 mV/decade), and reduced power dissipation [11]. However, the lower value of ON-current (I_{ON}) than conventional MOSFETs is a significant drawback of TFETs [12]–[15]. The different device architectures like vertical [16], [17], L-shaped or U-shaped [18], source-pocket structure [19] are widely used for improving the I_{ON}/I_{OFF}. Also, the fabrication of vertical TFET is straightforward to engineer compared to traditional TFETs [20]. Hence, source-pocket TFETs are found better in subthreshold characteristics than TFETs [21]. A lower bandgap material like germanium Ge and InAs are widely used in source-region to construct heterojunction TFET that can lower tunneling width and improve drain current owing to a rise in I_{OFF} ($\geq 10^{-12}$ A). The acquired value is higher than the maximum value of I_{OFF} of conventional Si-based TFETs [22]. In comparison to bandgap materials that are related to the III–V group, the staggered heterojunctions upon source-channel region were found suitable for lower-voltage operations with a trade-off of power consumption as well as device performance [23]. With such a viewpoint, a GaSb/Si heterojunction based V-DGTFET is designed to improve the device's power consumption. Therefore, the present work illustrates a label-free cavity on a half gate underlap and half gate overlap-based V-DGTFET biosensor. The device name describes that a cavity is made upon the source region which is in the tunneling area, thus improving the carrier concentration within the channel region. The presented structure has the potential to sense charged as well as neutral bioanalytes efficiently.

*The authors are with the Department of Electronics and Communication Engineering, National Institute of Technology, Patna, Bihar, 800005 India. E-mail: (at.phd20.ec@nitp.ac.in; meenap.ec@nitp.ac.in).

This article has been accepted for publication in IEEE Transactions on NanoBioscience. This is the author's version which has not been fully edited and content may change prior to final publication. Citation information: DOI 10.1109/TNB.2022.3183934

The biomolecules immobilization inside the nanogap cavity tends to change the oxide capacitance as demonstrated in device electrical characteristics. The different values of dielectric constants from 1 to 12 of biomolecules are considered to examine the performance of the device. Different biomolecules show efficiency to examine the energy band diagram, electric field, subthreshold swing, and drain current of a presented device [24]–[27]. The simulations for the V-DGTFET biosensor are carried out in the Silvaco ALTAS simulator [20].

For analyte sensing and stabilization, a key immobilization strategy is to directly link target particles to the necessary bioreceptors or the sensing surface. The label-free mechanism is precise and sensitive, and it allows for constant data monitoring to find the intrinsic properties of the target analyte. It only needs a single reagent that reduces the analysis time and cost compared to the labeled method [15]–[17]. In literature, different immobilization schemes preferred are adsorption, covalent-bond forming, cross-link method, and molecule entrapment [8]–[10]. The label-free mechanism shows immense potential for fabrication over micro-scale systems, thus providing better quality biosensors with high flexibility for remote diagnosis and other field applications. It needs to be insensitive to different physical parameters such as pH or environmental metrics [14]–[18]. Hence, the label-free method is a strong candidate for designing effective biosensors.

II. Device Architecture and Simulation Models

The GaSb/Si heterojunction based V-DGTFET biosensor with source pocket in the present paper is illustrated in Fig. 1(a). The fabrication flow for V-DGTFET biosensor is described in Fig. 1(b). Commonly, nanotechnology fabrication procedures are divided into bottom-up and top-down categories. In the top-down method, nanomaterials are produced by removing material from a bulk substrate until the required nanomaterial is achieved. The bottom-up method begins at the atomic or molecular level and progressively assembles the nanomaterial into the desired structure. The tentative fabrication process is based on the top-down approach for the proposed biosensor, in which the device was fabricated by using an n-type Si substrate [28]. The process can start with a drain metal on an n-type silicon layer. A thin ploy-Si metal layer was deposited on the Si substrate. The metal layer is exposed in the centre area, and silicon is again grown in that area. Next, the gate metal layer is deposited on the grown drain region by using Low-Pressure Chemical Vapor Deposition (LPCVD) at a low temperature and then etched out from the centre area. After that, SiO_2 and HfO_2 mask deposition on Si layers and then etch out from the centre area as well as the side portions to create a cavity in the proposed structure. After removing mask layers from the non-exposed area, the Si is again grown on that area, followed by the GaSb epitaxially grown on the silicon region. The final step in this fabrication process is to metallize the source electrode on the GaSb layer.

We calibrated the conventional vertical TFET with pocket [27] using TCAD simulation and reproduced the

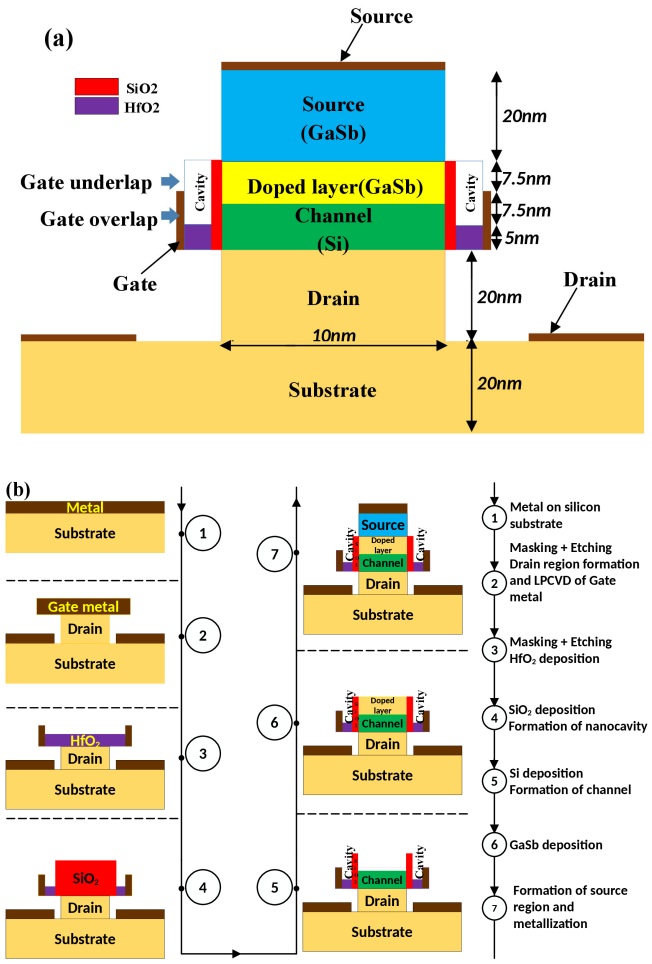

Fig. 1. Schematic illustration of (a) V-DGTFET biosensor (b) Fabrication process of V-DGTFET biosensor.

previously reported transfer characteristics, as shown in Fig. 2. Our structure includes the non-local band-to-band-tunneling (BTBT) model to account for local variation within the energy band to improve the device's tunneling efficiency. The lattice and thermal co-efficient mismatch between GaSb and Si lead to defects within GaSb-Si heterojunctions [10]. In consideration of this, in our structure, we included a non-locally trap-assistive model like TAT.NLDEPTH. The inclusion of these statements made results more appropriate. Along with, Shockley–Read–Hall (SRH) generation–recombination, field-dependent mobility, Auger recombination, Fermi–Dirac statistics and band gap-narrowing were included to improve the device performance. Further, to improve the fabrication compatibility and drain current, a high-k HfO_2 material (κ=25) is incorporated as a gate oxide in the present V-DGTFET biosensor [18], [26]. Also, the present V-DGTFET biosensor uses a lower channel length compared to all other biosensors. The different parameters utilized for device simulation are tabulated in Table I. The proposed structure design parameters are similar to the conventional model, except a nanocavity

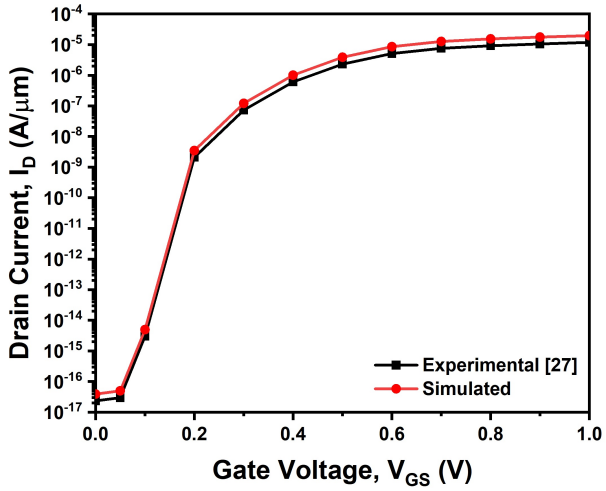

Fig. 2. Simulated output curves of conventional vertical TFET structure [27].

TABLE I. DESIGN PARAMETERS OF THE V-DGTFET.

Parameters	Values
Drain region concentration	1×10^{18} cm^{-3}
Source region concentration	1×10^{19} cm^{-3}
Channel concentration	1×10^{16} cm^{-3}
Channel length	12.5 nm
Drain length	20 nm
Source length	20 nm
Oxide width (SiO_2 and HfO_2)	0.62 nm and 3.38 nm
Substrate thickness (T_{Si})	20 nm
Doped layer length (GaSb)	7.5 nm
Doped layer concentration	1×10^{16} cm^{-3}
Spacer thickness (L_{us} and L_{ud})	3 nm and 15 nm
Work function tunnelling gate metal	4.20eV
Length of cavity	15nm
Dielectric permitivity SiO_2	3.7
Dielectric permitivity HfO_2	25

(half gate underlap and half gate overlap) [29]–[32] is built to recognize the biomolecules. To represent that cavity is air-filled, suitable material incorporated in the nanocavity with a dielectric constant (κ) value of 1. It reveals that no biomolecule lies inside the cavity. Similarly, for showing a cavity filled with biological molecules, the dielectric constant value is enhanced as per the biomolecule nature (κ>1).

III. RESULTS AND DISCUSSION

The response of the V-DGTFET biosensor while sensing both neutral and charged biomolecules is analyzed in this section, corresponding to different characteristics like energy bands, electric field, potential profile & drain current. Further, the V-DGTFET biosensor is analyzed using two different FOM's, namely sensitivity and linearity [33]. To simulate the electrical parameters of the device, in the existence of neutral biomolecules, the bioanalytes dielectric constant inside the cavity (half of the gate underlap, i.e., open cavity, and half of the gate overlap, i.e., close regions) are considered. The effects of various biomolecules on device performance are computed by changing air (κ=1) inside the nanogap cavity underneath the source region with different values of dielectric constants (κ>1) and charge density (N_f = ± 10^{10} C cm^{-2} to 10^{12} C cm^{-2}).

A. Impact of the neutral biomolecules

The impact of the V-DGTFET biosensor on the energy band diagram for air and neutral biomolecules is illustrated in Fig. 3(a). When there is no cavity, there is no change in valence band and conduction band of the structure. However, the band bending occurs in valence and conduction bands when the cavities are included. It is seen that while forming cavities, there is an improvement in barrier width separating the valence band and conduction band, which results in a lower electron tunneling probability and conduction current. Thus, it is observed that as the value of the dielectric constant [17] increases, there is a rise in band-bending that lowers the barrier width. Fig. 3(a) shows variation in energy band diagram concerned to neutral biomolecule (κ =1 to 12) at cavity length of 15 nm. The improvement in the dielectric constant value for biomolecules inside nanogap causes an increase in the hole density of the source region [19]. This layer of holes beneath the cavity in the source region improves the alignment of the valance band and conduction band. This reduced tunneling barrier enhances the electron's tunneling rate. Therefore, a rise in the tunneling causes an improvement in the device ON-current. The influence of neutral biomolecules on device drain

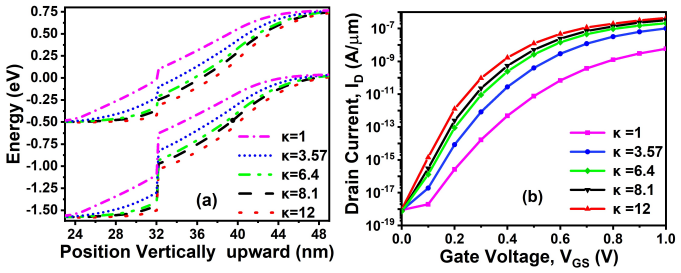

Fig. 3. (a) Energy band diagram (b) I_{DS}–V_{GS} characteristics at various dielectric constants, of the V-DGTFET biosensor with cavity length of 15 nm.

current characteristics is depicted in Fig. 3(b). A increase in the biomolecule's dielectric constant causes a reduction in the width of the tunneling barrier, as seen earlier, and thus rises the probability of tunneling and drain current reflected by equation (1). Therefore, the drain current variations sense the presence of biomolecules.

$$I_D \propto exp\left[-\frac{4\sqrt{2m^*}\,E_g^{*\frac{3}{2}}}{3|e|\hbar\left(E_g^*+\Delta\phi\right)}\sqrt{\frac{\varepsilon_{si}}{\varepsilon_{ox}}\,t_{ox}t_{si}}\right]\Delta\phi \qquad (1)$$

where e is the charge of electron, m^* is effective carrier mass, E_g^* is semiconductor material bandgap near tunnelling region, and ε_{si} and ε_{ox} are the dielectric constants of semiconductor and gate insulator, respectively. ΔI_{Drain} represents the variation in drain current in equation (2) when different type of neutral bioanalytes introduces in the cavity region.

$$\Delta I_{Drain} = I_{Drain}\,(bio-molecule) - I_{Drain}\,(air) \qquad (2)$$

This article has been accepted for publication in IEEE Transactions on NanoBioscience. This is the author's version which has not been fully edited and content may change prior to final publication. Citation information: DOI 10.1109/TNB.2022.3183934

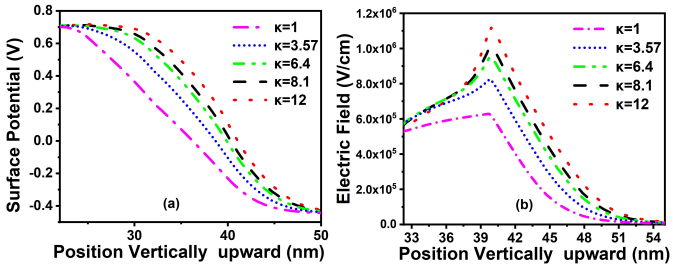

Fig. 4. (a) Surface potential (b) Electric field variations of V-DGTFET biosensor for various dielectric constants (no charge densities).

The impact of variations on the potential profile of the V-DGTFET biosensor concerning different κ-values of neutral biomolecules is demonstrated in Fig. 4 (a). With an increase in the dielectric constant value of biomolecules inside the cavity region, gate capacitance will increase. The effective gate capacitance [12] is proportional to the dielectric constant of neutral biomolecules in the nanocavity region, as shown in equation (3). It increases due to the enhanced fringing field with an increase in the dielectric constant of biomolecules inside the cavity region.

$$C_{eff} = \frac{\varepsilon_{SiO_2}\varepsilon_{bio}}{\varepsilon_{bio}t_{SiO_2} + \varepsilon_{SiO_2}t_{bio}} \tag{3}$$

where ε_{bio}, ε_{SiO_2} are the permitivities of the biomolecules and SiO_2 layer respectively having corresponding thicknesses t_{bio}, t_{SiO_2} respectively.

This gate capacitance increases gradually toward oxide capacitance because the inversion charge is not located exactly at the silicon-oxide interface, but at some depth that varies with gate voltage. As illustrated in Fig. 4 (a), a higher dielectric constant for biomolecules means a higher gate capacitance, a lower potential drop across the gate capacitance, and a higher potential under the oxide-silicon interface [34]. Hence, an improvement in device potential induces a downward shift in the energy band diagram, as shown in Fig. 3 (a). This decreases the width of the tunneling barrier, thus improving tunneling probability.

Fig. 4 (b) represents variations in electric field components of the V-DGTFET biosensor concerning various dielectric constants [24]. The electric field improves at the tunneling junction due to the formation of a steep doping profile with an increase in the dielectric constant values of neutral biomolecules in the cavities. At the tunneling junction, an electric field of 1.16×10^6 V/cm can be achieved for κ=12. This electric field increases the rate of vertical tunneling and drain current with an increase in the value of biomolecule's dielectric constant. From Fig. 4 (b) it is also observed that as the value of the dielectric constant decreases, the electric field decreases as well [15].

Fig. 5 depicts the variations in transconductance of the V-DGTFET biosensor concerning various dielectric constants for neutral biomolecules. It is realized that the transconductance of the V-DGTFET biosensor increases with increase in the dielectric constant value. From Figs. 6 (a) and 6 (b), it is observed that by reducing the thickness of the nanocavity region, both drain current and transconductance increase. In

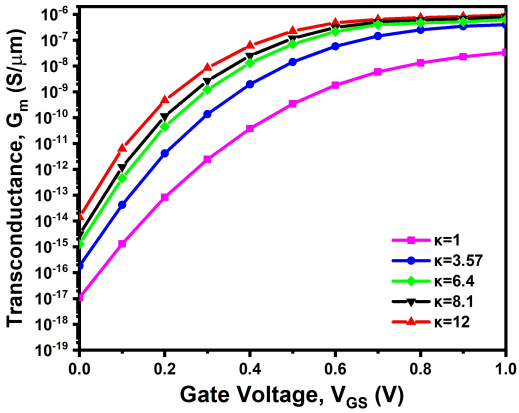

Fig. 5. Transconductance at V_{DS} = 0.5 V of the V-DGTFET biosensor for different neutral charged bio-molecules

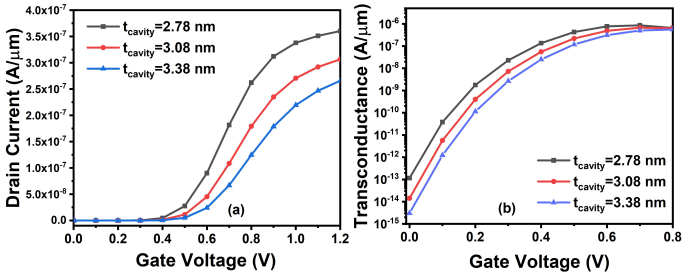

Fig. 6. (a) Drain current (b) Transconductance variations of V-DGTFET biosensor with respect to thickness of nanocavity.

this proposed device, 0.5 nm EOT is considered for SiO_2, i.e., 0.5 nm EOT is equivalent to 3.38 nm of HfO_2 [40]. Thus, the highest transconductance is obtained with a cavity thickness of 3.38 nm. The peak transconductance value rises with increasing κ-value of biomolecules. Δg_m represents the variation in transconductance in equation 3 when different neutral bioanalytes are introduced in the cavity region.

$$\Delta g_m = g_m\,(bio-molecule) - g_m\,(air) \tag{4}$$

B. Impact of the charged biomolecules

The impact of the V-DGTFET biosensor on the energy band diagram for charged biomolecules is illustrated in Fig.7(a). On immobilizing the biomolecules which are negatively (positively) charged within the cavity, an improvement (reduction) is found in the tunneling barrier width between valence and conduction band. The figure shows that tunneling barrier width is enhanced with a rise in positive charge density, which generally influences the electrons by decreasing the number of holes within the source-channel region. Thus, the control of the gate-channel region decreases if the positively energized biomolecules are inserted within the cavity. The abrupt doping between source channel appears with an increase in negatively energized biomolecules. Thus, the tunneling barrier width decreases for negatively charged biomolecules.

The dielectric constant affecting variances of charged biomolecules for cavity thickness value of 3.38 nm on the

This article has been accepted for publication in IEEE Transactions on NanoBioscience. This is the author's version which has not been fully edited and content may change prior to final publication. Citation information: DOI 10.1109/TNB.2022.3183934

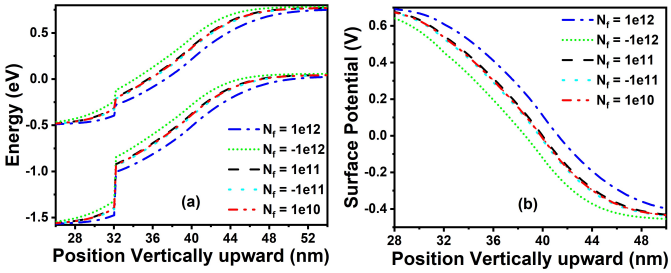

Fig. 7. (a) Energy band diagram (b) Potential Variation of the V-DGTFET biosensor at different charged biomolecules filled inside cavity of length 15 nm.

potential profile has been plotted in Fig.7(b). The present paper will analyze the potential by varying charge density from zero (neutral) to -1 × 10^{12} C cm^{-2} and 1 × 10^{12} C cm^{-2}. A potential change is achieved on immobilizing the biomolecules which are negatively charged within the cavity, i.e., from N_f = 1×10^{10} C cm^2 to -1×10^{12} C cm^2 (for κ = 8.1). As already seen in the energy band diagram (Fig. 7(a)) that shows the charge densities that affect flat band voltage as well as effective gate voltage. An increase in flat band voltage (V_{fb}) reduces the effective gate bias and surface potential for negatively charged biomolecules while increasing the tunneling width, as illustrated in Fig. 7(a) and 7(b). Hence, it leads to lower tunneling probability and reduced drain current. Similarly, the surface potential increases on immobilizing the positively charged biomolecules within the cavity, i.e., from N_f = 1×10^{10} C cm^2 to 1×10^{12} C cm^2 with neutral bio-molecules lying in the cavity (κ = 8.1). In contrast, Fig. 7(a) and 7(b) depict an opposite behavior showing the rise in positive charge density following a reverse process.

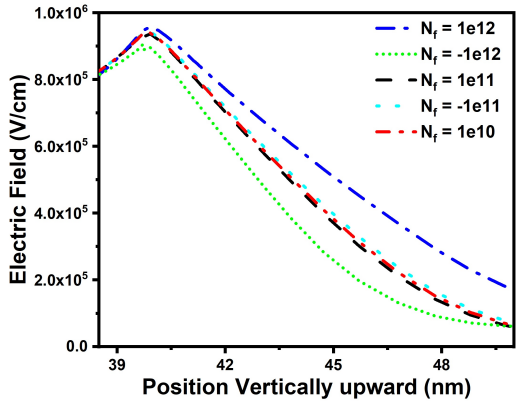

Fig. 8. Electric field variation of V-DGTFET biosensor at different value of charged densities i.e. ρ = 0 *to* − 1 × 10^{12} C cm^2 and 0 to 1×10^{12} C cm^{-2}.

The effect of charged (positive and negative) biomolecules on the device's electric field variations are illustrated in Fig. 8. From the figure, it is noticed that a rise in the positive charge density of biomolecules decreases the electric field with expanded tunneling barrier width, which enhances tunneling probability. Similarly, a rise in the negative charge density enhances the electric field, that reduces tunneling probability. The drain current characteristics of V-DGTEFT biosensor for charged biomolecules at κ=8.1 is shown in Fig. 9. From the figure, it is illustrated that device OFF current (I_{OFF}) decreases/increases corresponding to negatively/positively charged bioanalytes compared to neutral biomolecules. For increasing negative/positive charge within cavity [18], the barrier height of source-channel regime increases/decreases corresponding to reduction/rise in device drain current. Additionally, the device threshold voltage (V_{th}) enhances with a rise in the κ-value of target bioanalytes.

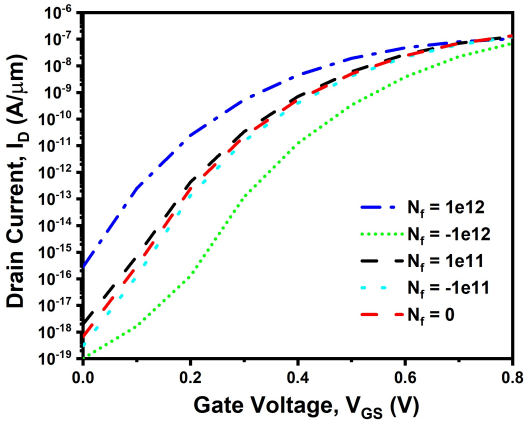

Fig. 9. I_{DS}–V_{GS} characteristics of the V-DGTFET biosensor at fixed value of dielectric constants, κ=8.1 and different value of charged densities i.e. ρ = 0 *to* − 1 × 10^{12} C cm^2 and 0 to 1×10^{12} C cm^{-2}.

C. Sensitivity analysis of drain current and transconductance

While analyzing the sensitivity of the V-DGTFET biosensor, the biomolecules are considered to exist within the nanogap. Fig. 10 reveals the sensitivity analysis of drain current concerning the gate voltage for various neutral biomolecules within the nanocavity regions at V_{DS} = 0.5 V. When the nanogap is filled with air, it can reproduce the response of the biosensor to sense the biomolecules. Thus, it is chosen as a reference to estimate sensitivity of the biosensors [24]–[26]. Hence, the sensitivity of a biosensor can be calculated as

$$S_{Drain\ \ Current}(\%) = \left(\frac{I_D^{bio} - I_D^{air}}{I_D^{air}}\right) * 100 \qquad (5)$$

where I_D^{bio} is the drain current value during cavity loaded with biomolecules and I_D^{air} is the drain current value during cavity loaded with air respectively. From Fig. 10, it is realized that the drain current sensitivity increases with the increase in the value of the dielectric constant(κ). The increase in the κ value of biomolecules reduces the device tunneling barrier length, which causes an improvement in the probability of tunneling. Thus, it increases the drain current, which generally senses the appearance of biomolecules.

The characteristics of transconductance sensitivity of the V-DGTFET biosensor with respect to gate voltage at various dielectric constants are reported in Fig.11. It is realized that the transconductance sensitivity is high for a low value of gate voltage, but if we increase the gate voltage further, sensitivity starts reducing exponentially. Due to lower values of gate voltage, the variation in the transconductance is significant, as

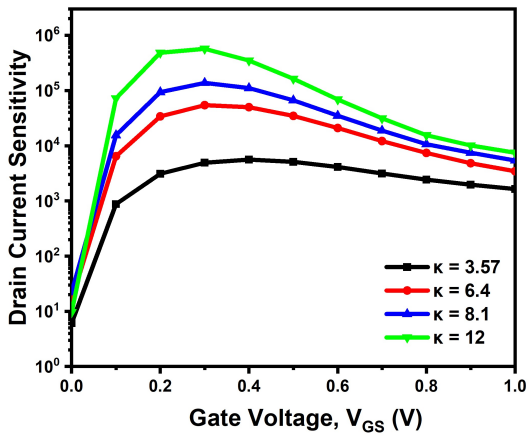

Fig. 10. Drain current sensitivity variation w.r.t V_{GS} at various dielectric constants and no charge density of V-DGTFET biosensor.

depicted in Fig. 5. For the voltage values about 1 V, a negligible variation is found in the transconductance value [23]. As the value of κ increases, the transconductance of the device increases, which enhances transconductance sensitivity. The following equation is used to compute transconductance sensitivity.

$$S_{transconductance}\,(\%) = \left(\frac{g_m^{bio} - g_m^{air}}{g_m^{air}}\right) * 100 \qquad (6)$$

where, g_m^{bio} is the transconductance value during cavity loaded with biomolecules, g_m^{air} is the transconductance value during cavity loaded with air respectively.

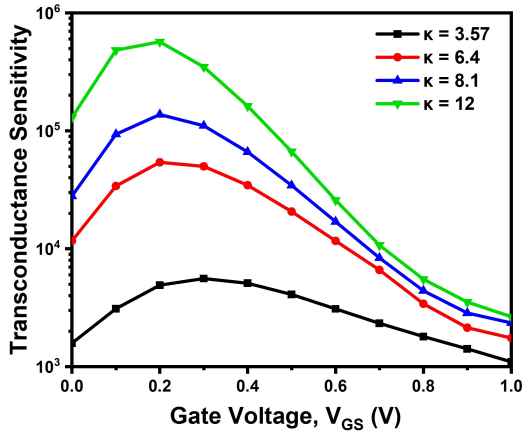

Fig. 11. Transconductance sensitivity variation w.r.t V_{GS} at various dielectric constants and no charge density of V-DGTFET biosensor.

Table II depicts the performance of various TFET-based biosensors. It can give a comparative analysis about how biosensors can work competently on a specific scope of operations based on the sensitivities of FET-based biosensors. Also, it shows the advantage that the V-DGTFET biosensor has over them due to the different dimension ratios, materials, and dielectric constant of bioanalytes.

TABLE II. Investigation of Published TFET Based Biosensor's Performance

Sl.No.	Title of FET Based Biosensors	Sensitivity Parameter	Sensitivity
1.	DM PNPN TFET with 0% Ge [26]	Drain Current	4×10^3
2.	DM PNPN TFET with 10% Ge [26]	Drain Current	6×10^3
3.	DM PNPN TFET with 20% Ge [26]	Drain Current	5×10^3
4.	DG TFET [34]	Drain Current	1.05×10^2
5.	Nanowire TFET [35]	Drain Current	9×10^3
6.	DM JLTFET [36]	Drain Current	1.9×10^4
7.	DM DG TFET [37]	Drain Current	2.84×10^5
8.	Full Gate DM TFET [38]	Drain Current	1×10^5
9.	DM FET [39]	Drain Current	3×10^4
10.	V-DGTFET [This Work]	Transconductance and Drain Current	5.8×10^5 and 5.6×10^5

D. Effect of biomolecules control embedded in nanocavity on device characteristics

The inbuilt nanocavity to immobilize biomolecules is assumed to be fully filled for detecting biomolecules. Still, many unfilled spaces are detected within the cavity area while testing various target bio-analytes [18]. Due to these vacant spaces within the cavity, there exists a variation in the device's electrical characteristics compared to expected characteristics. Hence, we consider another parameter to detect sensitivity, such as biomolecule occupancy (γ_{Bio}) within the nanocavity. The number of biomolecules filled within the cavity region (in %) given by γ_{Bio} and is defined as

$$\gamma_{bio} = \frac{\text{Thickness of filled cavity}}{\text{Total cavity thickness}} \times 100 \qquad (7)$$

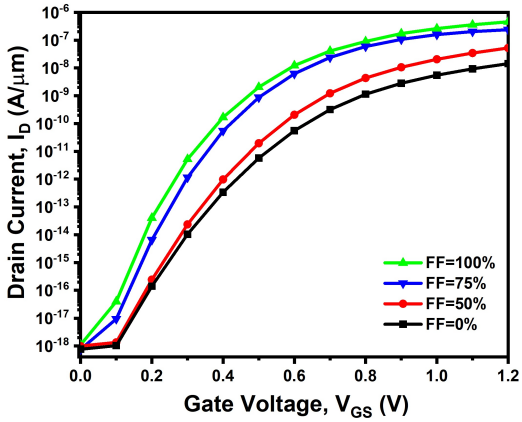

Fig. 12. Variation in drain characteristics of the V-DGTFET biosensor w.r.t V_{GS} when cavity is filled with neutral biomolecules (FF= 0% to 100%) at cavity length of 15 nm.

Fig. 12 reveals the biosensor transfer characteristics with cavity thickness of 3.38 nm and dielectric constant of 8.1 corresponds to various biomolecule occupancies. We analyzed four configurations for occupancies including 0 %, 50 %, 75 % and 100 %. To study the influence of the fill factor, the cavity

is filled up with biomolecules to a certain height while the rest is kept empty or air-filled. An increase in biomolecule occupancy in the cavity region from 0% to 100% of the proposed structure directly influences the gate capacitance. For uniform distribution of biomolecules, certain sections of the cavity are completely filled with biomolecules, while others are vacant. Due to the uniform biomolecule distribution, two parallel capacitances are formed in the cavity region [12], which are represented by equations (8) and (9).

$$C_{eff1} = \frac{\varepsilon_{SiO_2}\varepsilon_{bio}}{\varepsilon_{bio}t_{SiO_2} + \varepsilon_{SiO_2}t_{bio}}, \ cavity\ with\ biomolecules \quad (8)$$

$$C_{eff2} = \frac{\varepsilon_{SiO_2}\varepsilon_{air}}{\varepsilon_{air}t_{SiO_2} + \varepsilon_{SiO_2}t_{air}}, \ cavity\ filled\ with\ air \quad (9)$$

where ε_{bio}, ε_{SiO_2}, ε_{air} are the permitivities of the biomolecules, SiO_2 layer and air gap respectively having corresponding thicknesses t_{bio}, t_{SiO_2}, t_{air} respectively.

From the equations, it is observed that effective gate capacitance is directly proportional to the dielectric constant of neutral biomolecules in the nanocavity region. An increase in the number of biomolecules that occupy the cavity will enhance the dielectric constant and capacitance. This leads to a reduction in the length of the tunneling barrier, which causes an improvement in the tunneling probability. Hence, as the value of biomolecule occupancy increases, drain current increases.

E. Linearity analysis of V-DGTFET based biosensor

One of the most significant figures of merit in biosensors is linearity. The linearity of the biosensor describes its ability to react to the variations reliably across different measurements. It can be expressed as the equation $y = mc$, where y is the output signal, c is the concentration of the analyte and m is the sensitivity of biosensor. In the present study linearity of the V-DGTFET biosensor is tested for drain current and transconductance shifts [26]. The equation of linearity [33]

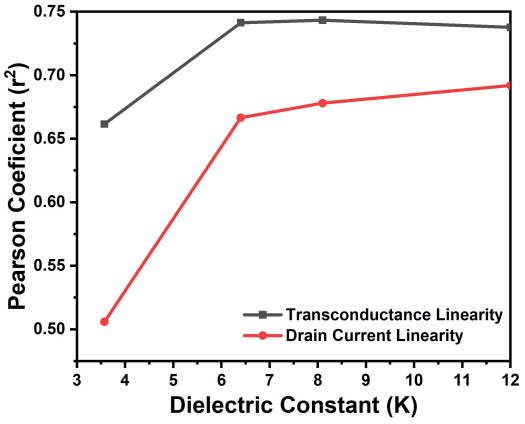

Fig. 13. Variations in pearson coefficient (r^2) of the V-DGTFET biosensor w.r.t different value of dielectric constant for drain current and transconductance linearity.

for drain current and transconductance sensitivities are given by *Drain Current=slope[κ]+drain current at κ=1* and *Transconductance=slope[κ]+transconductance at κ=1*. Here linearity is closely relates to the degree of fitness, which is computed using pearson's coefficient (r^2). Variations in the Pearson coefficient (r^2) with respect to different values of the dielectric constant for drain current and transconductance linearity are shown in Fig. 13. This fitness coefficient for the present structure is given by $r^2 \geq 0.75$(κ=8.1) (transconductance sensitivity), $r^2 \geq 0.70$(κ=8.1) (drain current sensitivity). Hence, it is observed that the V-DGTFET biosensor is better in terms of linearity.

IV. Conclusion

The present work provides a novel structure of V-DGTFET biosensor for label-free detection of biomolecules. The detection of various (both neutral and charged) biomolecules is carried out proficiently by V-DGTFET label-free biosensor. The performance is analyzed using FOMs such as sensitivity and linearity by changing the charge density and dielectric constant. The electrical metrics such as energy band diagram, transfer characteristics, surface potential, transconductance, and electric field are studied with variations of neutral and charged biomolecules inside the cavity. The optimum value of transconductance and drain current sensitivity is obtained by this model 5.8×10^5 and 5.6×10^5, respectively. On analyzing the electrical parameters and device immunity for SCEs, the V-DGTFET biosensor is a proficient biosensor in detecting charged/neutral biomolecules. The obtained transconductance sensitivity of 5.8×10^5 that comes 14%, 22%, and 39% more in comparison to apomyoglobin (κ =8.1), bacteriophage-T7 (κ =6.4), and APTES (κ =3.57) sensitivity at 15 nm cavity length.

References

[1] A.P.F. Turner, I. Karube, G.S. Wilson, Biosensors: Fundamentals and Applications, Oxford University Press, Oxford Oxfordshire; New York, 1987.

[2] T.C. Lim, Nanosensors: Theory and Applications in Industry, Healthcare, and Defense, Crc Press, Boca Raton, 2011.

[3] A.W. Dey et al., "High-current GaSb/InAs(Sb) nanowire tunnel field-effect transistors," IEEE Electron Device Lett., vol. 34, no. 2, pp. 211–213, Feb. 2013.

[4] C. Dincer, R. Bruch, E. Costa-Rama, M.T. Ferna´ndez-Abedul, A. Merkoc¸i, A. Manz, G.A. Urban, F. Gu¨der, Disposable sensors in diagnostics, food, and environmental monitoring, Adv. Mater. (2019) 1806739.

[5] Girish Wadhwa, Balwinder Raj, "Design, Simulation and Performance Analysis of JLTFET Biosensor for High Sensitivity," IEEE Transactions on nanotechnology, vol. 18, pp. 567-574, 2019.

[6] Wadhera, T., Kakkar, D., Wadhwa, G., Raj, B. (2019). Recent advances and progress in development of the field effect transistor biosensor: A review. Journal of Electronic Materials, 48(12), 7635-7646.

[7] Ajay, Student, Rakhi Narang, Manoj Saxena and Mridula Gupta, "Modeling and Simulation Investigation of Sensitivity of Symmetric Split Gate Junctionless FET for Biosensing Application," IEEE Sensors Journal, vol. 17, no. 15, pp. 4853-4861, June 2017.

[8] S. Chander et al., "Two-dimensional analytical modeling for electrical characteristics of Ge/Si SOI-tunnel FinFETs," Superlattices Microstructures, vol. 131, pp. 30–39, Jul. 2019.

[9] C. Convertino, C. B. Zota, H. Schmid, A. M. Ionescu, and K. E. Moselund, "III–V heterostructure tunnel field-effect transistor," J. Phys., Condens. Matter, vol. 30, Jun. 2018, Art. no. 264005.

[10] H. Uchida, T. Soga, H. Nishikawa, T. Jimbo, and M. Umeno, "Reduction of dislocation density by thermal annealing for GaAs/GaSb/Si heterostructure," J. Cryst. Growth, vol. 150, pp. 681–684, May 1995.

[11] Chusovitin, S. Dotsenko, S. Chusovitina, and D. Goroshko, "Formation of a thin continuous GaSb film on Si (001) by solid phase epitaxy," Nanomaterials, vol. 8, no. 12, p. 987, 2018.

[12] R. Narang, M. Saxena, and M. Gupta, "Comparative analysis of dielectric-modulated FET and TFET-based biosensor," IEEE Trans. Nanotechnol., vol. 14, no. 3, pp. 427–435, May 2015.IEEE Transaction on Electron Devices, vol. 59, no. 10, pp. 2809-2817, Oct. 2012.

[13] W. Tanu, ,. G. Wadhwa, T. Bhardwaj and D. K. Balwi, "Design and Performance Analysis of Symmetrical and Asymmetrical Triple Gate Dopingless Vertical TFET for Biorecognition," Silicon, pp. 1-9, 2020.

[14] G. Wadhwa, J. Singh and B. Raj, "Design and investigation of doped triple metal double gate vertical TFET for performance enhancement," Silicon, pp. 1-11, 2020.

[15] M. Patil, A. Gedam and G. P. Mishra, "Performance Assessment of a Cavity on Source ChargePlasmaTFET-Based Biosensor," in IEEE Sensors Journal, vol. 21, no. 3, pp. 2526-2532, 1 Feb.1, 2021.

[16] N. Kannan and M. J. Kumar, "A Drain-side Gate-underlap I-MOS (DGI-MOS) transistor as a label-free biosensor for detection of charged biomolecules," in Proc. 2nd Int. Conf. Emerg. Electron., 2014, pp. 1–4

[17] Mahalaxmi, B. Acharya and G. P. Mishra, "Design and Analysis of Dual-Metal-Gate Double-Cavity Charge-Plasma-TFET as a Label Free Biosensor," in IEEE Sensors Journal, vol. 20, no. 23, pp. 13969-13975, 1 Dec.1, 2020.

[18] M. Verma, S. Tirkey, S. Yadav, D. Sharma and D.S. Yadav, "Performance assessment of a novel vertical dielectrically modulated TFET-based biosensor," IEEE Trans. Electron Devices, vol. 64, no. 9, pp. 3841-3848, Sep. 2017.

[19] Narang, R., Saxena, M., Gupta, R.S. and Gupta, M., 2011. Dielectric modulated tunnel field-effect transistor—A biomolecule sensor. IEEE electron device letters, 33(2), pp.266-268.

[20] Atlas User's Manual Silvaco Int. Softw., Silvaco Inc., Santa Clara, CA, USA, 2016.

[21] Bhattacharyya, A., Chanda, M. and De, D., 2019. Performance assessment of new dual-pocket vertical heterostructure tunnel FET-based biosensor considering steric hindrance issue. IEEE Transactions on Electron Devices, 66(9), pp.3988-3993.

[22] Wadhwa, G. and Raj, B., 2018. Parametric variation analysis of symmetric double gate charge plasma JLTFET for biosensor application. IEEE Sensors Journal, 18(15), pp.6070-6077.

[23] Narang, R., Reddy, K.S., Saxena, M., Gupta, R.S. and Gupta, M., 2012. A dielectric-modulated tunnel-FET-based biosensor for label-free detection: Analytical modeling study and sensitivity analysis. IEEE transactions on electron devices, 59(10), pp.2809-2817.

[24] Y. Khatami and K. Banerjee, Steep subthreshold slope n-and p-type tunnel-FET devices for low-power and energy-efficient digital circuits, IEEE Transactions on Electron Devices, 56(11), pp.2752-2761, 2009

[25] R. Goswami and B. Bhowmick, "Dielectric-Modulated TFETs as LabelFree Biosensors," in Design, Simulation and Construction of Field Effect Transistors, vol. 1, IntechOpen, Ed. DhanasekaranVikraman, 2018,Ch. 2,pp. 17-35,doi: 10.5772/intechopen.76000.

[26] S. Kanungo, S. Chattopadhyay, P. S. Gupta, K. Sinha, and H. Rahaman, "Study and analysis of the effects of SiGe source and pocket-doped channel on sensing performance of dielectrically modulated tunnel FETbased biosensors," IEEE Trans. Electron Devices, vol. 63, no. 6, pp. 2589–2596, Jun. 2016.

[27] Tripathy, M. R., Singh, A. K., Samad, A., Chander, S., Baral, K., Singh, P. K., Jit, S. (2020). Device and circuit-level assessment of GaSb/Si heterojunction vertical tunnel-FET for low-power applications. IEEE Transactions on Electron Devices, 67(3), 1285-1292.

[28] K. Vanlalawmpuia and B. Bhowmick, "Analysis of Hetero-Stacked Source TFET and Heterostructure Vertical TFET as Dielectrically Modulated Label-Free Biosensors," in IEEE Sensors Journal, vol. 22, no. 1, pp. 939-947, 1 Jan.1, 2022.

[29] Ye, Shujun Yamabe, Kikuo Endoh, Tetsuo. (2019). Variance Reduction during the Fabrication of Sub-20 nm Si Cylindrical Nanopillars for Vertical Gate-All-Around Metal-Oxide- Semiconductor Field-Effect Transistors. ACS omega. 4. 10.1021/acsomega.9b02520.

[30] Lee, Khwang-Sun Park, Jun-Young. (2022). N-Type Nanosheet FETs without Ground Plane Region for Process Simplification. Micromachines. 13. 432. 10.3390/mi13030432.

[31] Harris, Harlan Choi, Kisik Mehta, Nirvesh Chandolu, A. Biswas, Nabin Kipshidze, G. Nikishin, S. Gangopadhyay, S. Temkin, H.. (2002). HfO2 gate dielectric with 0.5 nm equivalent oxide thickness. Applied Physics Letters. 81. 1065-1067.

[32] Guerfi, Y., Larrieu, G. (2016). Vertical silicon nanowire field effect transistors with nanoscale gate-all-around. Nanoscale research letters, 11(1), 1-7.

[33] N. Shafi, A. M. Bhat, J. S. Parmar, C. Sahu and C. Periasamy, "Analytical Modeling of Surface Potential and Figure of Merit Computation for Planar Junctionless pH Sensing BioFET," in IEEE Transactions on Nanotechnology, vol. 20, pp. 534-542, 2021.

[34] V. D. Wangkheirakpam, B. Bhowmick and P. D. Pukhrambam, "N+ Pocket Doped Vertical TFET Based Dielectric-Modulated Biosensor Considering Non-Ideal Hybridization Issue: A Simulation Study," in IEEE Transactions on Nanotechnology, vol. 19, pp. 156-162, 2020.

[35] D. Sarkar and K. Banerjee, "Proposal for tunnel-field-effect-transistor as ultra-sensitive and label-free biosensors," Appl. Phys. Lett., vol. 100, no. 14, Apr. 2012, Art. no. 1431083.

[36] Wadhwa, G., Raj, B. Label Free Detection of Biomolecules Using Charge-Plasma-Based Gate Underlap Dielectric Modulated Junctionless TFET. Journal of Elec Materi 47, 4683–4693 (2018).

[37] A. Anam, S. Anand and S. I. Amin, "Design and Performance Analysis of Tunnel Field Effect Transistor With Buried Strained Si1xGex Source Structure Based Biosensor for Sensitivity Enhancement," in IEEE Sensors Journal, vol. 20, no. 22, pp. 13178-13185, 15 Nov.15, 2020.

[38] S Kanungo, S. Chattopadhyay, P. S. Gupta, and H. Rahaman, "Comparative performance analysis of the dielectrically modulated full-gate and short-gate tunnel FET-based biosensors," IEEE Trans. Electron. Devices, vol. 62, no. 3, 994–1001, Mar. 2015.

[39] H Im, X.-J. Huang, B. Gu, and Y.-K. Choi, "A dielectric-modulated field effect transistor for biosensing," Nature Nanotechnology, vol. 2, no. 7, pp. 430–434, Jun. 2007.

[40] W. Park, A. N. Hanna, A. T. Kutbee and M. M. Hussain, "In-Line Tunnel Field Effect Transistor: Drive Current Improvement," in IEEE Journal of the Electron Devices Society, vol. 6, pp. 721-725, 2018.